

Asynchronous Distributed Bayesian Optimization at HPC Scale

Romain Egelé
*Université Paris-Saclay, France &
Argonne National Laboratory, USA*
romainegele@gmail.com

Joceran Gouneau
*INP-ENSEEIH, France &
Argonne National Laboratory, USA*
joceran.gouneau@etu.toulouse-inp.fr

Venkatram Vishwanath
*Leadership Computing Facility
Argonne National Laboratory, USA*
venkat@anl.gov

Isabelle Guyon
*CNRS/Inria-LISN
Université Paris-Saclay, France*
guyon@chalearn.org

Prasanna Balaprakash
*Mathematics and Computer Science Division &
Leadership Computing Facility
Argonne National Laboratory, USA*
pbalapra@anl.gov

Abstract—Bayesian optimization (BO) is a widely used approach for computationally expensive black-box optimization such as simulator calibration and hyperparameter optimization of deep learning methods. In BO, a dynamically updated computationally cheap surrogate model is employed to learn the input-output relationship of the black-box function; this surrogate model is used to explore and exploit the promising regions of the input space. Multipoint BO methods adopt a single manager/multiple workers strategy to achieve high-quality solutions in shorter time. However, the computational overhead in multipoint generation schemes is a major bottleneck in designing BO methods that can scale to thousands of workers. We present an asynchronous-distributed BO (ADBO) method wherein each worker runs a search and asynchronously communicates the input-output values of black-box evaluations from all other workers without the manager. We scale our method up to 4,096 workers and demonstrate improvement in the quality of the solution and faster convergence. We demonstrate the effectiveness of our approach for tuning the hyperparameters of neural networks from the Exascale computing project CANDLE benchmarks.

Index Terms—machine learning, Bayesian optimization, asynchronous, parallel

I. INTRODUCTION

Black-box optimization seeks to optimize a function based solely on input-output information. This problem is of particular interest in many scientific and engineering applications and is quite relevant to several machine learning tasks. In the former case, the optimized black box is often the result of a complex simulation code, software, or workflow where we can get only the output for a given input configuration. In the latter, many learning algorithms are sensitive to hyperparameters, which cannot be inferred during the training process and often need to be adapted by the user based on the training data [1]. Existing methods for solving black-box optimization can be grouped into model-based and model-free methods. In the former, a surrogate model for the black-box function is learned in an online fashion and used to speed up the search. Examples include trust-region methods [2], sequential model-based optimization [3], [4], and estimation of distribution

methods [5]. In the latter, the search navigates the search space directly without any explicit model. Examples include Nelder-Mead methods [6], particle swarm optimization [7], cross-entropy methods [8], variants of evolutionary algorithms [9], random search, and simulated annealing [10]. These two groups of methods have their own strengths and weaknesses. A key advantage of model-based over model-free methods is the search efficiency. Given an explicit model, the search can quickly identify promising regions of the search space and find high quality solutions faster than model-free methods can [11]. Bayesian optimization (BO) is a promising class of sequential-model-based optimization methods. It has been used in a wide range of black-box function optimization tasks [11], [12], [13]. In BO, an incrementally updated surrogate model is used to learn the relationship between the inputs and outputs during the search. The surrogate model is then used to prune the search space and identify promising regions. BO navigates the search space by achieving a balance between exploration and exploitation to find high-performing configurations. While the exploration phase samples input configurations that can potentially improve the accuracy of the surrogate model, the exploitation phase samples input configurations that are predicted by the model to be high performing.

With the transition of high-performance computing (HPC) systems from petascale to exascale [14], massively parallel Bayesian optimizations that can take advantage of multiple computing units to perform simultaneous black-box evaluations are attractive. These methods will be particularly beneficial for many HPC use cases, such as simulator calibration, software tuning, automated search of machine learning pipelines, neural network hyperparameter tuning, and scientific simulation optimization. Nevertheless, the inherent sequential nature of BO [15], [3], [16], [17] presents challenges for scaling. Most of the parallel Bayesian optimization methods propose a multipoint acquisition strategy in a centralized architecture where the manager performs BO and workers evaluate the black-box functions. Also, these methods often use Gaussian process as surrogate model [11], [18]. However,

these two components respectively the centralized architecture and the GPR are two major bottlenecks for scaling BO in an HPC setting.

To sum up, the problem we seek to solve is to **improve both quality of the final solution and time to solution of black-box optimization problems**, by efficiently using a **fixed number of workers computing in parallel**. To that end, we develop a parallel BO method involving a **decentralized architecture** without a single manager. Each worker runs its own BO and **communicates asynchronously** its black box evaluation results with other workers. Additionally, each worker performs **asynchronous surrogate model updates**, using the **effective qUCB acquisition function** (previously proposed in a centralized context to effectively navigate search space). Our original contribution is to combine these 3 key ingredients (decentralized, asynchronous communication/updates, and qUCB acquisition function) in a powerful parallel BO method that beats the state-of-the-art significantly by finding better solutions in shorter computational time. As a side contribution, we gain additional improvements by adapting the computational effort of the surrogate model updates, when it enters a more expensive regime approaching the effort of computing a new point of the black box model it tried to approximate in a cheap way. This situation was unprecedented in BO because never enough points were calculated to make this an issue.

Our principal findings support the effectiveness of our method:

- Faster convergence and better solution over state-of-the-art distributed synchronous BO methods [19], [20] on standard continuous black-box benchmark functions.
- Faster convergence and better solution for neural networks hyperparameter tuning from the Exascale computing project CANDLE benchmarks over asynchronous centralized BO methods based on Gaussian process regression and pruning [21], [22].
- Scaling studies of parallel BO methods at HPC scale involving 4,096 workers, a scale never been reported in the BO literature.

II. RELATED WORK

Most parallel BO methods follow a centralized single manager/multiple workers [11] approach, where a manager runs the BO and generates configurations sequentially [23], [24], and the workers evaluate the configurations and send the results back to the manager. The manager generates configurations in a batch synchronous or asynchronous way [25]. Many methods make use of Gaussian process regression (GPR) because it can provide gradients for optimization methods used in selecting the most informative configurations for evaluation. Although these methods have achieved considerable success, they are often limited to small HPC resources with tens of parallel workers. By design, centralized BO is not a scalable approach because a single manager managing requests from many workers can create congestion and, therefore, increase the worker idle time, where the worker will be waiting for

the manager to suggest a configuration to evaluate. This issue will worsen with larger numbers of workers because GPR has a cubic time complexity [26] for model fitting and will significantly affect the scalability of the BO methods. In contrast to centralized search architectures, distributed BO was recently introduced based on stochastic policies such as Thompson sampling and Boltzmann policy [19], [20] (denoted by bUCB when applied to UCB) but restricting the study to synchronous communication, a dozen parallel workers and GPR. Instead of GPR, other surrogate models have also been investigated in the literature. These include Bayesian neural networks [27] and random forest [28] but were used only in sequential BO and batch synchronous single manager multiple worker schemes. They are also limited to 10s of parallel workers. We show that our proposed distributed BO with asynchronous communication will be able to scale better than that of the widely used centralized single manager/multiple worker parallelization schemes with GPR models.

III. BACKGROUND

A. Bayesian Optimization

Bayesian optimization is a well-established method to solve the global optimization problem of expensive and noisy black-box functions [29]. For a detailed overview see [11]. The problem we seek to solve is formally presented in Eq. 1:

$$\max_x \{f(x) : x = (x_{\mathcal{I}}, x_{\mathcal{R}}, x_{\mathcal{C}}) \in \mathcal{X}\}, \quad (1)$$

where $x = (x_{\mathcal{I}}, x_{\mathcal{R}}, x_{\mathcal{C}})$ is a vector of n_d parameters partitioned into three types of parameters \mathcal{I} , \mathcal{R} , and \mathcal{C} , respectively denoting discrete parameters with a natural ordering, continuous parameters taking real values, and categorical parameters with no special ordering; $f(x)$ is a *computationally expensive* black-box objective function that needs to be maximized (minimization problems can also be carried out similarly by changing the sign of f). Typically, the feasible set \mathcal{X} is defined by a set of constraints on the parameters x . This includes bound constraints that specify the minimum and maximum values for the parameters and linear and non-linear constraints that express the feasibility of the given parameter configuration through algebraic equations. Consequently, given these algebraic constraints, the time required to verify the feasibility (that is, if $x \in \mathcal{X}$) is negligible. Hidden constraints are unknown to the user and generally require a evaluation of the black-box function f to be uncovered. The objective function $f(x)$ can be deterministic (the same values $f(x)$ for the same x) or stochastic (different $f(x)$ values for the same x). Generally, finding the global optimal solution of the stated problem is computationally intractable [30], [13], [12], except for the simplest cases. The presence of integer and categorical parameters, algebraic and hidden constraints, results in a discontinuous parameter space, which makes the search process difficult. Several mathematical optimization algorithms take advantage of gradients that measure the change in the value of the objective function with respect to the change in the values of the parameters. This is not feasible for the

general problem 1, however, because the black-box function cannot be differentiated. We focus on the optimization problem setting where the black-box function f is computationally expensive to evaluate.

B. Surrogate Model

BO uses a computationally cheaper surrogate-model to provide new points for evaluation. The choice of a good surrogate model plays a crucial role in the scalability and effectiveness of the BO search method. In most BO methods, GPR is employed because of its built-in uncertainty quantification capability [11], [18]. Specifically, GPR implicitly adopts Bayesian modeling principles of estimating the posterior distribution of output from the given input-output pairs and provides the predictive mean and variance for the unevaluated input configurations. GPR also has the advantage of being differentiable. However, while GPR is superior for faster convergence when run sequentially it remains one of the key bottlenecks for computational scalability in HPC setting where thousands of input-output pairs (samples) can be computed in one batch. In fact, the GPR model needs to be refitted with a rapidly growing set of samples (past and new), but it has a cubic complexity $O(n_{\text{sample}}^3)$ [26] with respect to the number of samples n_{sample} . For a small n_{sample} , this is not an issue. At scale, however, the cubic time complexity for model fitting will slow or even stop the search’s ability to generate new input configurations, thus increasing the idle time of the workers and eventually resulting in poor HPC resource utilization as well as fewer overall evaluations. Other surrogate models were proposed in the literature such as deep neural networks [27] and random-forest regressor (RFR) [31], [28]. We adopt RFR for its wide adoption thanks to its versatility with real, discrete and categorical features as well as its robustness. RFR has a fitting time complexity of $O(n_{\text{tree}} \cdot n_{\text{feature}} \cdot n_{\text{sample}} \cdot \log(n_{\text{sample}}))$ with n_{tree} number of trees in the ensemble and n_{feature} number of features ($= n_d$, problem dimension) per sample, which is constant for each search setting. In addition to the log-linear time complexity, RFR provides simple and easy in-node parallelization opportunities, where each tree can be built independently of other trees in the ensemble.

C. Acquisition function

The way in which the input point x is selected for evaluation is another bottleneck for scalability. The selection method comprises an acquisition function that measures how good a point is and a selector that seeks to optimize the acquisition function over \mathcal{X} . Typically, when all the parameters are continuous (or if they afford such encoding/transformation), specialized gradient-based optimizers are employed to select the next point. However, because of the lack of a closed-form integral for RFR, the mixed-integer nature of the parameter space, the presence of algebraic constraints, and the resulting discontinuity in the search space, such optimizers cannot be employed. While specialized mixed-integer nonlinear solvers for these types of problems do exist, they are computationally expensive and cannot be employed in the fast iterative context

required for scaling. Therefore, we use a point selection scheme that uses an upper confidence bound (UCB) [11] acquisition function on top of a random sample from \mathcal{X} . This scheme selects an input point x for evaluation as follows. A large number of unevaluated configurations are sampled from the feasible set \mathcal{X} . The BO uses a dynamically updated surrogate model m to predict a point estimate (mean value) $\mu(x)$ and variance $\sigma(x)^2$ for each sampled configuration x . The sampled configurations are then ranked using the UCB given by

$$\text{UCB}(x) = \mu(x) + \kappa \cdot \sigma(x), \quad (2)$$

where $\kappa \geq 0$ is a parameter that controls the trade-off between exploration and exploitation. When κ is set to zero, the search performs only exploitation (greedy); when κ is set to a large value, the search performs stronger exploration. A balance between exploration and exploitation is achieved when κ is set to an appropriate value, classically $\kappa = 1.96$, which translates into a 95% confidence interval around the mean estimate when computing UCB.

IV. PROPOSED METHOD

In this section we introduce our novel approach to BO in the context of HPC exploiting a distributed architecture with asynchronous communication. In fact, multiple compute units can be used on an HPC platform, where each function evaluation requires a fraction of this platform. Let n_{worker} be the number of available workers, where a worker represents a unit of computational resource available to evaluate the black-box function (e.g., CPU, GPU, fraction of a compute node, whole node or a group of nodes). Let T_{wall} be the total wall-clock time for which these resources are available (i.e., job duration). Then the overall available compute time $T_{\text{avail}} = n_{\text{worker}} \cdot T_{\text{wall}}$ upper bounds the total time spent in black-box function evaluations $T_{\text{eff}} = \sum_{t_{\text{eff}} \in \mathcal{T}} t_{\text{eff}}$ used to perform the job, where \mathcal{T} is the set of durations t_{eff} for all evaluated black-box functions. We define “effective utilization” as $U_{\text{eff}} = T_{\text{eff}}/T_{\text{avail}}$. For the problem of “parallel black-box optimization” we seek to maximize the objective function f , as well as maximize the effective utilization U_{eff} . We maximize the later by minimizing the computational overhead of the search algorithm. In other words, in addition to the objective function maximization, the optimization method should effectively use parallel resources by maximizing their usage mainly with black-box evaluations.

BO is a promising approach for tackling the class of black-box optimization problems described in Eq. 1. BO tries to leverage accumulated knowledge of f throughout the search by modeling it as a probability distribution $p(y|x)$, which represents the relationship between x , the input, and y , the output. Typically, BO methods rely on dynamically updating a surrogate model that estimates $p(y|x)$. Often, this distribution is assumed to follow a normal distribution. Therefore, the surrogate model estimates both $\mu(x)$ the mean estimate of y and $\sigma(x)^2$ the variance. The latter is leveraged to assess how uncertain the surrogate model is in predicting x [11]. The

surrogate model is cheap for prediction and can be used to prune the search space and identify promising regions, where the surrogate model is then iteratively refined by selecting new inputs that are predicted by the model to be high performing (exploitation) or that can potentially improve the quality of the surrogate model (exploration). BO navigates the search space by achieving a balance between exploration and exploitation to find high-performing input configurations.

A. Asynchronous Distributed Bayesian Optimization

Figure 1b shows a high-level sketch of our proposed asynchronous distributed Bayesian optimization (ADBO) method. The key feature of our method is that each worker executes a sequential BO search; performs only one black-box evaluation, which avoids congestion occurring in a centralized setting (see Fig. 1a); and communicates the results with all other workers in an asynchronous manner. The BO of each worker differs from that of the other workers with respect to the value κ used in the acquisition function UCB. Each BO starts by sampling the value κ_i from an exponential distribution $\text{Exp}(\frac{1}{\kappa})$, where κ is the user-defined parameter. The BO that takes smaller κ_i values will perform exploitation and sample points near the best found so far in the history H . On the other hand, the BO that receives large κ_i values will perform exploration to reduce the predictive uncertainty of the RFR model. Consequently, on average multiple BO searches will seek to achieve a good trade-off between exploration and exploitation; however, there will be a number of BO searches that perform stronger exploitation or exploration. This effect will increase as we scale to a large number of workers and can benefit the overall search. Our approach is inspired by the qUCB acquisition function [32] for the single manager/multiple workers setting, where different κ values are sampled from the exponential distribution for the UCB acquisition function and different points are selected based on these values to find the balance between exploration and exploitation. The main reason for adopting qUCB is computational simplicity. Compared to other multipoint generation strategies, such as the constant liar [33] (denoted by CL) that exist in the single-manager/ multiple-worker methods, there is no significant overhead to achieve a balance between exploration and exploitation.

Algorithm 1 shows the high-level pseudocode of our proposed ADBO method. The worker uses the history H , a data structure that keeps track of the input-output pairs seen by it and other workers. The search proceeds by initializing the optimizer object with a randomly sampled κ_i value from an exponential distribution; the search is implemented through ask-and-tell interfaces. The former implements the acquisition function and selector functionality and is used to generate an input x_i for the evaluation of the black-box function. The latter is used to give the evaluation results and retrain the RFR surrogate model. As soon as the black-box evaluation is completed, the `send_all` function is used to send the (x, y) to all other workers. Next the `recv_any` function is used to read the evaluations results from a local worker-specific buffer that stores the results from all other workers. Both `send_all`

and `recv_any` are asynchronous; the former does not wait for the acknowledgment of other workers, and the latter does not wait for all workers to send their most recent results. The history H is then updated with other workers' input-output pair along with the current (x, y) pair. The updated history is then used to refit the surrogate model through the tell interface.

Algorithm 1: Asynchronous Distributed Bayesian Optimization (Worker Process)

Inputs : f : black-box function, κ : UCB hyperparameter, $comm$: communicator
Output: H the history of evaluated configurations
 /* Initialization */
 1 $H \leftarrow \text{History}()$ */
 2 $\kappa_i \sim \text{Exp}(\frac{1}{\kappa})$
 3 $optimizer \leftarrow \text{Optimizer}(\kappa_i)$
 /* Main loop */
 4 **while not done do**
 5 | $x \leftarrow optimizer.ask()$
 6 | $y \leftarrow f(x)$
 7 | `send_all` $(x, y, comm)$
 8 | $H \leftarrow \text{recv_any}(H, comm)$
 9 | `optimizer.tell` (H)
 10 **end**

B. Improved uncertainty quantification in random forest

Although RFR provides computational advantages, its uncertainty quantification capabilities are not well known or documented in the literature. The most widely used RFR implementation is from the Scikit-Learn package [34]. Our analysis of uncertainty quantification with the default implementation of this package showed that the predictive variance is not as good as that of GPR. The primary reason was the best-split strategy adopted in the usual random forest algorithm to minimize the variance of the estimator. Although this results in better predictive accuracy, the predictive variance is not informative in the context of Bayesian optimization because it is constant in unexplored areas. We tested the random split strategy for tree splitting, as documented in [28], and found that the uncertainty estimates from RFR are improved and are comparable to those with GPR. But because it does not follow the conventional RF algorithm, the split strategy was not exposed as a parameter to the user. We believe that this might be one of the reasons that RFR, despite its computational advantages, was not thoroughly experimented with for the purpose of uncertainty quantification. The uncertainty of the RFR is computed by applying the law of total variance on the mean estimate $\mu_{\text{tree}}(x)$ and variance estimate $\sigma_{\text{tree}}(x)^2$ of the trees of the ensemble, which are learned by minimizing the squared error:

$$\sigma(x)^2 = \mathbb{E}[\sigma_{\text{tree}}(x)^2] + \mathbb{V}[\mu_{\text{tree}}(x)], \quad (3)$$

where $\mathbb{E}[\cdot]$ and $\mathbb{V}[\cdot]$ are respectively the empirical mean and variance. Our new implementation of RFR with its improved uncertainty estimate module will be made available as open source software for future research.

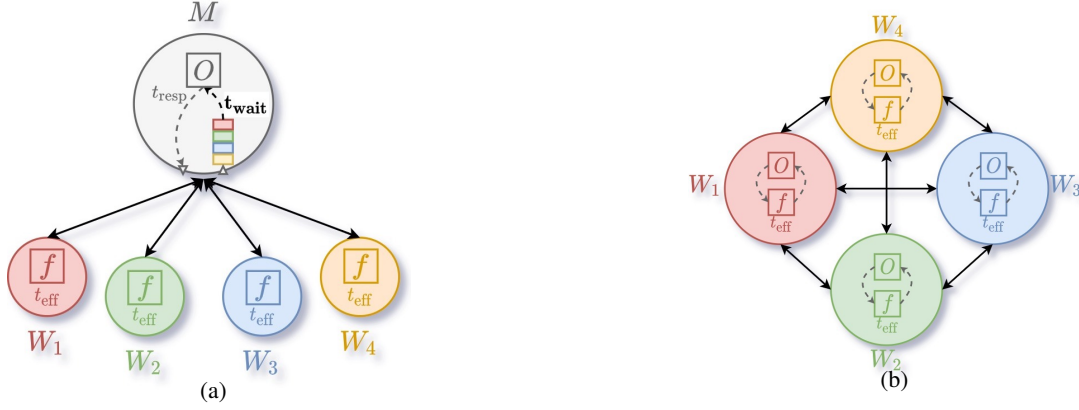


Fig. 1: Centralized (1a) and distributed (1b) search models. A circle represents a process with W for a worker and M for a manager, an arrow represents a communication, O represents the optimizer, and f represents the computation of the black-box function. t_{wait} is the time for which a worker waits before being processed by the optimizer. t_{resp} is the time taken by the optimizer to suggest a new configuration.

C. Reducing refitting complexity of the surrogate model

Despite the log-linear time complexity, RFR surrogate model training can become computationally expensive as the search progresses. The reason is that at each refit step, the RFR model needs to be retrained from scratch with the entire set of collected input-output pairs (x, y) that the search has so far acquired. This becomes an issue at scale because the larger the number of workers, the faster the value of n_{sample} will grow and increase the refitting time. Therefore, we reduce the refitting time complexity by using two methods. First, we upper-bound the number of samples n_{sample} to a constant value $n_{\text{max_sample}}$ by quantile-based undersampling, where we define five equal-spaced quantiles on the set of collected objective values (using 6 intervals) and sample with replacement $n_{\text{max_sample}}/5$ points for each interval. The quantile-based undersampling provides a mechanism to reduce input points that have similar output values. While it is possible that a large number of points will be left out at a given refit step, all the points in the history have a positive probability of re-sampled again for the next fit. This also allows our BO method to look at different regions of the input space at different steps. Second, instead of using the default n_{feature} for the split in the tree construction, we use $\log_2(n_{\text{feature}})$; this is useful for problems with large dimensions. Consequently, the complexity of RFR refit will become bounded by $O(n_{\text{tree}} \cdot \log_2(n_{\text{feature}}) \cdot n_{\text{max_sample}} \cdot \log(n_{\text{max_sample}}))$.

D. Implementation-specific details

Algorithm 2: Sending Function (`send_all`)

Inputs : *comm*: communicator, *x*: configuration, *y*: objective value

```

1 requests ← []
2 for i ← 1 to comm.size() do
3   if i ≠ comm.rank() then
4     | requests.push(comm.isend(i, (x, y)))
5   end
6 end
7 waitall(requests)

```

Algorithm 3: Receive Function (`recv_any`)

Inputs : *comm*: communicator, *H*: history of evaluated configurations

Output: *H*: updated history

```

1 N ← 0
2 received_any ← (comm.size() > 1)
3 while received_any do
4   /* Emit requests */
5   received_any ← False
6   requests ← []
7   for i ← 1 to comm.size() do
8     if i ≠ comm.rank() then
9       | requests.push(comm.irecv(i))
10    end
11  end
12  /* Process requests */
13  for i ← 1 to comm.size() - 1 do
14    if requests[i].done then
15      | H.push(requests[i].data)
16      | N ← N + 1
17      | received_any ← True
18    end
19    requests[i].cancel
20  end
21 end

```

The details of the `send_all` and `recv_any` functions are shown in 2 and 3, respectively. The algorithms use primitives from the Message Passing Interface [35] (MPI). The `send_all` function uses the MPI `isend` asynchronous primitive to send the evaluation results (i.e., input-output pair) to other workers. The `recv_any` function uses the MPI `irecv` asynchronous primitive to receive the data previously sent by other workers. The *comm* variable is in charge of connecting the different processes of the current execution. In `send_all` (Alg. 2) we emit all asynchronous sending requests that are nonblocking (1.1–6). The current process waits for the completion of these requests (1.7) to make sure the data is sent. Then, in `recv_any` (Alg. 3) we start by setting a condition (1.2) to enter the following loop only if there are at least two workers. Subsequently, we enter the

loop (l.3), which will be repeated until no additional data is received, a process that is managed with the *received_any* variable. Afterwards, inside the loop we have a first block (l.4–10) that emits asynchronous receive worker at once (i.e., without blocking) and a second block between (l.11–18) that processes the requests by updating the history H with received data (l.13) when a request has been completed (l.12) or cancels the request otherwise (l.17) to avoid blocking and continue. This procedure should minimize the idle time of a worker and therefore increase utilization.

V. EXPERIMENTS

First, we systematically evaluate our proposed ADBO method with qUCB (ADBO+qUCB) against the state-of-the-art distributed BO (SDBO+bUCB) on a number of commonly used benchmark functions found in the literature. Since two components differs between the methods (A vs. S and q vs. b), we conduct experiments to show the advantages of each components of the proposed ADBO+qUCB method, such as asynchronous communication (A vs. S), distributed search (D vs. C), and the acquisition function (qUCB vs. bUCB or CL). Finally, we apply our method ADBO+qUCB to the problem of tuning of hyperparameters of a deep neural network model training.

The first set of experiments is conducted on the Theta supercomputer at the Argonne Leadership Computing Facility (ALCF). Theta is a Cray XC40 that comprises 4,392-nodes, each equipped with a 64-core Intel Knights Landing processor with 16 GB of MCDRAM in-package memory and 192 GB of DDR4 memory. The compute nodes are interconnected by using an Aries Dragonfly network with a file system capacity of 10 PB. In this part, each worker is attributed 2 cores. The second set of experiments, with hyperparameter tuning, is conducted on ThetaGPU, another system at the ALCF. ThetaGPU comprises 24 NVIDIA DGX A100 nodes, each equipped with eight NVIDIA A100 Tensor Core GPUs, two AMD Rome CPUs of 64 cores, 320 GB of GPU memory. and 1 TB of DDR4 memory. In this part, each worker is attributed 1 GPU. All experiments when repeated once are performed with the same initial random state 42. The algorithm is implemented in Python 3.8 where the main packages used are mpi4py 4.0.0, scikit-learn 1.0.1 and a fork from scikit-Optimize. The RFR is from scikit-learn with a modified split rule. Neural networks are implemented in Tensorflow 2.8.

A. Comparison with the state-of-the-art distributed synchronous BO

In this section, to test our idea of using asynchronous communication with qUCB, we compare our proposed ADBO+qUCB with a recently developed *synchronous* distributed BO (SDBO) with *Boltzmann policy* on top of the UCB acquisition function (bUCB) (fully denoted as SDBO+bUCB) [20] on a number of commonly used benchmark functions¹. These include 10-dimensional Ackley,

Griewank, Levy, and Schwefel functions and a 6-dimensional Hartmann6D function. All these are minimization problems. We emulate the computationally expensive function f by artificially setting the compute time of the black-box evaluation by sampling a time from a normal distribution $\mathcal{N}(\mu = 60s, \sigma = 20s)$. This simulates the variation of the run time of a black-box function f such as neural networks with different training times or simulators with input-dependent run times. Both ADBO+qUCB and SDBO+bUCB use the RFR in our experiments. Every BO runs with a given wall time of $T_{wall} = 25$ minutes. We used 128 workers for both search methods. Figure 2 shows the search trajectories of the ADBO+qUCB and SDBO+bUCB methods, where the best-found solutions over the search time are plotted. From the results we can observe that our proposed ADBO+qUCB outperforms the state-of-the-art SDBO+bUCB method with respect to both solution quality and search time. ADBO+qUCB finds high-quality solutions in shorter search time, and on all the benchmarks the final solution found by ADBO is superior to that of SDBO+bUCB. This improvement is attributed to two factors: first, the asynchronous nature of ADBO+qUCB results in 1.68x more function evaluations on average than that of SDBO+bUCB; and second, the use of Boltzmann policy for the acquisition function was not as effective as the qUCB used in ADBO+qUCB.

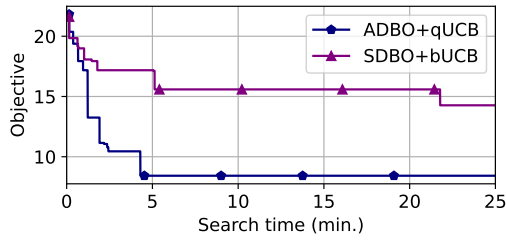
B. Impact of scaling ADBO workers

In this section, we scaled the ADBO+qUCB and SDBO+bUCB methods from 128 workers to 4,096 workers on the benchmark functions. As a default we ran ADBO+qUCB without the two surrogate model refitting complexity reduction strategies (feature reduction and quantile-based undersampling). The results are shown in Fig. 3 for a 5-dimensional Ackley function. Each experiment is repeated 5 times with different random-states and we plot the average and standard-error over these repetitions. We observe a positive impact of scaling on the quality of the solution. Increasing the scale increases the ability of ADBO+qUCB to find high-quality solutions in short computation time, as shown in Fig. 3a. With respect to the number of black-box evaluations performed by the ADBO+qUCB method, we can observe a linear scaling up to 2,048 workers; however, the scaling drops at 4,096 workers. Similarly, the effective utilization starts from 0.93 for 128 workers and drops to 0.86 and 0.77 for 2,048 and 4,096 workers, respectively. We found that this result is not due to communication overhead. In fact, the communication is still negligible at this scale, but the time required for RFR model retraining becomes a bottleneck. In particular, as the search progresses, with an increased scale the number of input-output pairs increases drastically, which increases the model retraining time. While the SDBO+bUCB method also achieves a linear scaling trend similar to ADBO+qUCB’s, the number of function evaluations is much lower, which can be attributed to synchronization and the consequent low effective utilization of 0.5 across different numbers of workers.

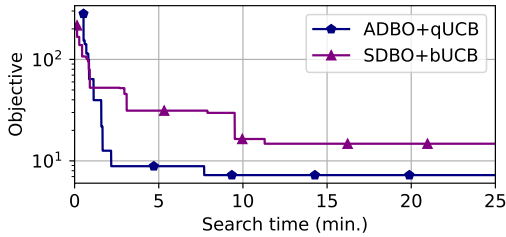
¹<https://www.sfu.ca/~ssurjano/optimization.html>

C. Impact of scaling problem dimensions

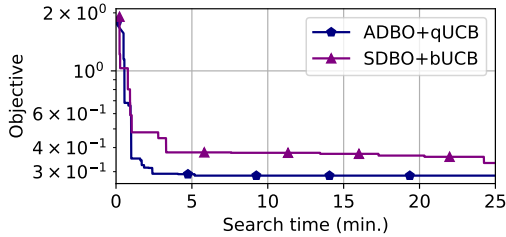
In this section, we analyze the effect of increasing the size of the input dimension on ADBO+qUCB’s effective utilization.



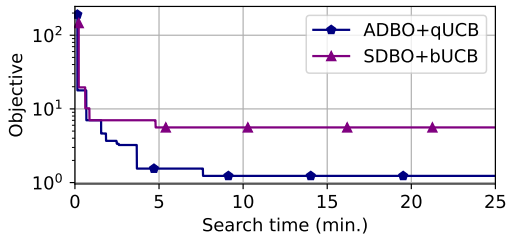
(a) Ackley



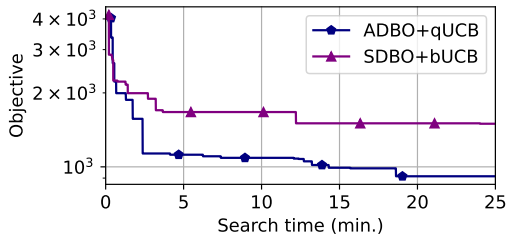
(b) Griewank



(c) Hartmann6D

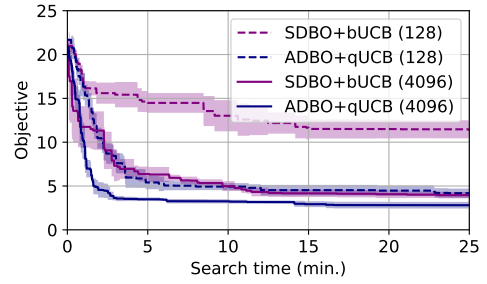


(d) Levy

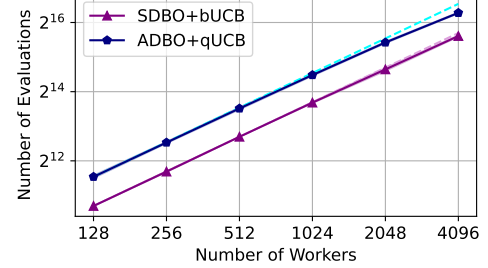


(e) Schwefel

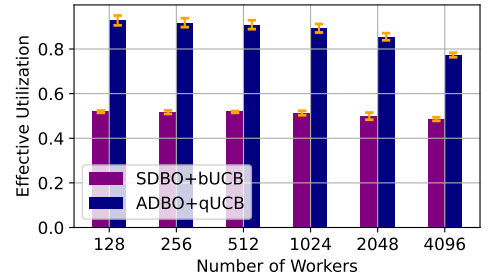
Fig. 2: Comparison of asynchronous distributed with qUCB (ADBO+qUCB) and synchronous distributed with Boltzmann policy (SDBO+bUCB) for different benchmark functions.



(a) The search trajectory showing the best objective found over time



(b) The strong scaling with respect to the number of function evaluations



(c) Effective utilization of workers

Fig. 3: Comparison of ADBO+qUCB (blue) and SDBO+bUCB (purple) for a growing number of parallel workers.

We increase the dimensions of the Ackley function from 5, 10, 30, 50, and 100 with 4,096 parallel workers. We compare ADBO+qUCB, which uses all the input features and all collected samples, with its optimized variant ADBO+qUCB+frqs (feature reduced and quantile sampling), which reduces the refitting complexity of the RFR model. The upper bound on the number of samples is set to n_{\max_sample} to 5,000.

The results are shown in Fig. 4. For ADBO+qUCB, we can already observe in the workers’ scaling results (Fig. 3b) that a loss of performance starts to be noticed at the 4,096 workers scale. In fact, the effective utilization is less stable in this setting with the quickly increasing quantity of samples that progressively slows the refitting of the surrogate model. When scaling the number of dimensions, this phenomenon is even worse, as shown, and utilization drops from about 75% with 5 dimensions, to 49% with 30 dimensions, and to 15% with 100 dimensions. In fact, an increase of n_{feature} quickly slows the refitting of the surrogate model. In contrast, if we look at the optimized version ADBO+qUCB+frqs, we can observe that the drop of utilization is amortized without being stopped. It brings up the utilization from 75% to 80% with 5 dimensions,

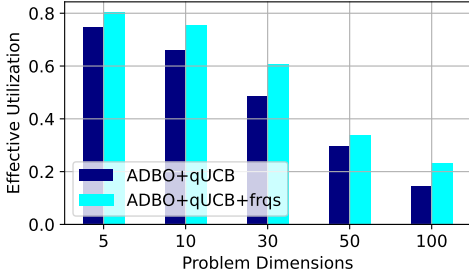


Fig. 4: Comparison of ADBO+qUCB and ADBO+qUCB+frqs (feature reduction and quantile-based undersampling) effective utilization when scaling the dimensionality of the problem.

from 49% to 60% with 30 dimensions, and from 15% to 23% with 100 dimensions. In conclusion, the feature reduction with quantile undersampling provides a solution to amortize the drop of performance when scaling the dimensionality of the search space.

D. Componentwise evaluation

In this section we evaluate the impact of the various ingredients of our proposed method ADBO+qUCB on performance. We start with a simple BO baseline, then progressively introduce the algorithmic components of our method. We use the 5-dimensional Ackley benchmark function. This function is particularly interesting because it contains many local optima and a unique global optimum $f(0, \dots, 0) = 0$. It is often used to test the effectiveness of optimizers in escaping a local minimum.

1) *Batch synchronous vs. asynchronous in centralized setting*: In this section we evaluate the advantage of asynchronicity. For this we start with a classic baseline, centralized BO (CBO) method. In this case, a “manager” runs the search and generates configurations for evaluation, and workers evaluate them and return the results to the manager. A common method for generating multiple configurations is the constant liar (CL, also known as Kriging believer) method, where after selecting a first configuration x_0 , the model is refitted with the maximum objective known so far (lie) for x_0 before selecting the next configuration x_1 . This process is repeated until the number of required points is selected. Thus, to generate p points, the BO needs to refit the model $p - 1$ times sequentially. Within CBO, two schemes are widely used in the literature: batch synchronous and asynchronous. In the batch synchronous version, we need to wait for all parallel evaluations to complete before iterating, which is adapted when the run time of the black-box evaluations is almost constant. In the asynchronous version, we resample a new configuration as soon as a worker becomes free, which is adapted when the run time of the black-box function varies. We refer to these methods as SCBO+CL and ACBO+CL, respectively. As a baseline, we use the vanilla sequential BO, referred as SEQ-1, which evaluates configurations one at a time and uses a single worker.

The results are shown in Fig. 5. We can observe that ACBO+CL finds high-quality solutions in shorter computation time when compared with SCBO+CL and SEQ-1 (Fig. 5a). A

key reason is the better worker utilization, as seen in Fig. 5b, where we observe that the batch synchronous scheme can significantly reduce the overall worker utilization. The effective utilization U_{eff} is 0.16 for SCBO+CL and 0.22 for ACBO+CL, which results in a total of 508 and 686 function evaluations, respectively. However, we notice that the expensive refit of the surrogate model in the constant liar strategy prevents the search from scaling well to a higher number of workers. In conclusion, asynchronicity improves performance but constant liar is a bottleneck for better performance.

In order to address the overhead issue of the constant liar and the model refitting schemes, several multipoint acquisition strategies have been proposed. We compared two low-overhead strategies, Boltzmann policy with UCB (denoted as bUCB) and qUCB, with the default constant liar strategy (denoted as CL) within the asynchronous centralized search setting (ACBO). Boltzmann policy transforms the vector of scores from the acquisition function into a categorical distribution [20] from which we can sample configurations. The Boltzmann operator is a generalization to the Softmax operator where the entropy of the categorical distribution can be managed by a temperature parameter. The temperature can be chosen according to a specific schedule such that convergence is maintained while exploration is ensured asymptotically [20]. We observed that ACBO+qUCB and ACBO+bUCB outperformed ACBO+CL with respect to both worker utilization and solution quality.

2) *Asynchronous centralized vs distributed search*: Here we compare ACBO+qUCB (centralized) and our proposed

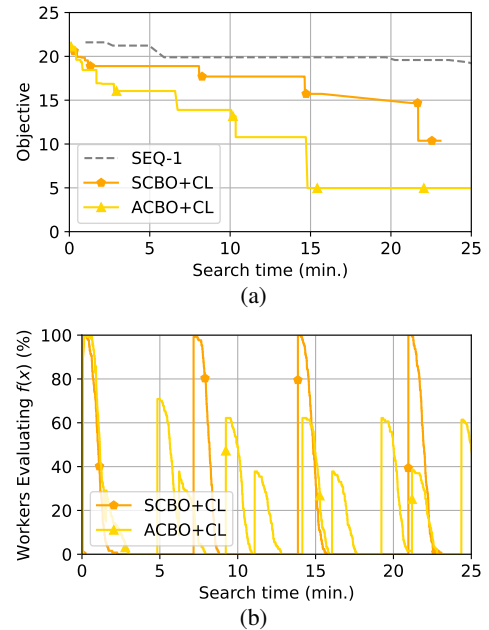
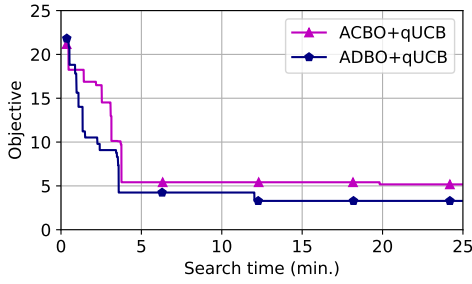
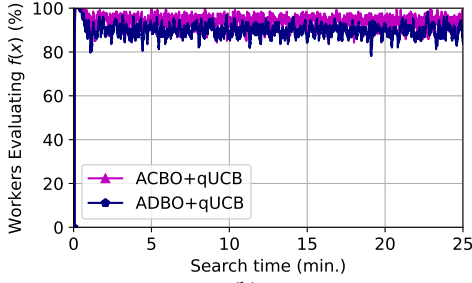


Fig. 5: Comparison of the sequential (SEQ-1, grey), synchronous (SCBO+CL, orange), and asynchronous (ACBO+CL, yellow) centralized search with the constant liar strategy. On the top, the search trajectory (5a) and at the bottom the percentage of active workers (5b) are presented with respect to the time.



(a)

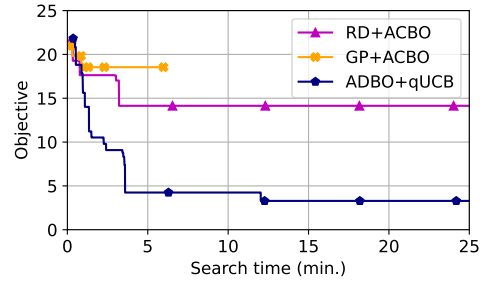


(b)

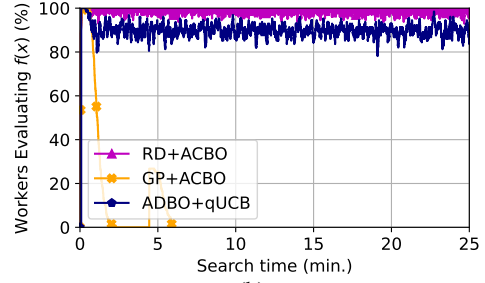
Fig. 6: Comparison of asynchronous centralized (ACBO+qUCB) and distributed (ADBO+qUCB) search with qUCB. On the top, the search trajectory (6a) is presented; at the bottom is shown the percentage of active workers (6b) with respect to time.

ADBO+qUCB (distributed) method and show that the latter is a promising alternative to the widely used single-manager parallel-BO approach. The results are shown in Fig. 6a. While the effective utilization of the two methods is comparable for 128 workers (see Fig. 6b), ADBO+qUCB achieves solutions that are better than those of ACBO+qUCB. The reason can be attributed to the BO search within each worker with κ values, which provides diversity in balancing the exploration and exploitation of the search space. Moreover, ADBO+qUCB takes advantage of an ensemble of RFR models as opposed to a single RFR model in ACBO+qUCB. The input-output samples collected through the ensemble of RFR models allow the search method to escape local solutions faster. As we scale, this feature will become more advantageous in finding high-quality solutions in a short computation time.

3) *Comparison with baselines:* We compare our BO method to two commonly used baselines to demonstrate the trade-off between the computational cost of the surrogate model and the number of black-box evaluations required for high solution quality. These baselines are random search (RD+ACBO) and BO with Gaussian Process (GP+ACBO), where both use centralized architecture. For GP+ACBO, the constant-liar scheme is used for multipoint generation. The search are performed with 4,096 workers. The results are shown in Fig. 7. From the results we can observe that ADBO+qUCB outperforms Random and GP with respect to both search time and solution quality. ADBO+qUCB reaches a better objective than the other two baselines within 3 min. We also observe that RD+ACBO obtains better solution than GP+ACBO and latter gets stuck at 6 min. The poor



(a)



(b)

Fig. 7: Comparison of asynchronous centralized random and Gaussian Process (GP) search with distributed (ADBO+qUCB) search with qUCB. On the top, the search trajectory (7a) is presented; at the bottom is shown the percentage of active workers (7b) with respect to time.

performance of GP+ACBO can be attributed to the large refitting time complexity associated with GPR. This is evident from the worker utilization results, where the BO with GPR cannot generate points rapidly enough to keep the workers busy. The search in BO with GPR did not progress after 6 min. because the rest of the time was spent in fitting the model. The high computational cost of refitting the GP model and the associated bottleneck at scale were reported in previous works as well [27], [21]. While RD+ACBO has a better utilization (0.96 with with 3,048 evaluations) than ADBO+qUCB (0.87 with 2,778 evaluations), the solution quality of latter is better than the former. Even if random search is a good to maximize utilization its probability of finding the optimal solution exponentially reduces with the number of dimensions for random-sampling. Let's take an example, for the Ackley function we want to evaluate the probability of finding ≈ 3.29 (found by ADBO+qUCB). There are 5-dimensions and the bounds are $(-32.768, 32.768)$. Assuming a uniform prior, the probability of sampling at ϵ -precision for 1 dimension is $p_\epsilon := P(x^* - \epsilon \leq X \leq x^* + \epsilon) = \frac{2\epsilon}{b-a}$. Now considering the sampling for each dimension to be independent, the probability of sampling at ϵ -precision each dimension for d -dimensions is $p_d := p_\epsilon^d$. Finally, assuming that draws are independent for each new evaluation, the probability of sampling at ϵ -precision each dimension after n -draws is $p_n := 1 - (1 - p_d)^n$. In our example, $f(x + 0.32) \approx 3.3$, therefore with $(a, b) = (-32.768, 32.768)$, $\epsilon = 0.32$, $d = 5$ and $n = 3048$ we have a probability of $p_n \approx 10^{-7}$ for Random to outperform ADBO+qUCB.

E. Application to neural network hyperparameter tuning

Here we demonstrate the effectiveness of ADBO+qUCB to tune the hyperparameters of neural networks. For this comparison we used DeepHyper [36] and Optuna [37] which are two state-of-the-art open source package for neural network hyperparameter optimization. DeepHyper adopts an asynchronous BO method [21] with a single manager and multiple workers with the UCB acquisition function and constant liar scheme for generating hyperparameter configurations for multiple workers simultaneously. It also provide us with common search methods such as random search and asynchronous BO with Gaussian Process (GP) search methods for hyperparameter tuning. We refer these two search methods as RD+ACBO and GP+ACBO because they both follow a centralized asynchronous architecture. DeepHyper has been used to improve the accuracy of neural networks in several scientific machine learning applications [38], [39], [40], [41]. In addition, we implemented an asynchronous variant of Hyperband (ASHA) [22], [42] based on the pruner API of the Optuna Python package. We selected two benchmarks, namely, Attn and Combo, from the Exascale Deep Learning and Simulation Enabled Precision Medicine for Cancer (EPC-CANDLE) project [43]. For both benchmarks we run the search on 64 workers (GPUs) for 3 hours. Each neural network is trained for 10-epochs with RD+ACBO, GP+ACBO, and ADBO+qUCB but a dynamic budget between 1 to 10-epochs is given for ASHA, which performs early pruning of poor performing configurations.

1) *Attn benchmark*: The Attn [44] benchmark dataset contains 271,915 training points and validation/testing 33,989 points. Each point is composed of 6,212 feature input and a binary output, representing a binary classification task. The total dataset is about 7.9 GB. The data suffers form a strong imbalance between positive and negative targets which is managed by a re-weighting of the loss. The baseline model is a feed-forward neural network with an attention layer. For the default neural architecture hyperparameters, there are layers which are all equipped with ReLU except the attention layer which uses softmax and with the number of neurons $\in [1000, 1000, 1000, 500, 250, 125, 60, 30]$. Each of these layer is followed by a batch-normalization and dropout which are not activated by default. The validation AU-ROC after 10-epochs is used as metric to guide the hyperparameter optimization. It reaches an AUC-ROC of 0.872.

The number of neurons and the activation function of each layer are exposed for hyperparameter tuning. The search space is defined as follows: number of neurons: [10, 1024] with a log-uniform prior; activation function: [elu, gelu, hard sigmoid, linear, relu, selu, sigmoid, softplus, softsign, swish, tanh]; optimizer: [sgd, rmsprop, adagrad, adadelata, adam]; global dropout-rate: [0, 0.5]; batch size [8, 512] with a log-uniform prior; and learning rate: $[10^{-5}, 10^{-2}]$ with a log-uniform prior. This corresponds to 17 hyperparameters.

The results are shown in Fig. 8. From the search trajectory shown in Fig. 8a we observe that our proposed ADBO+qUCB

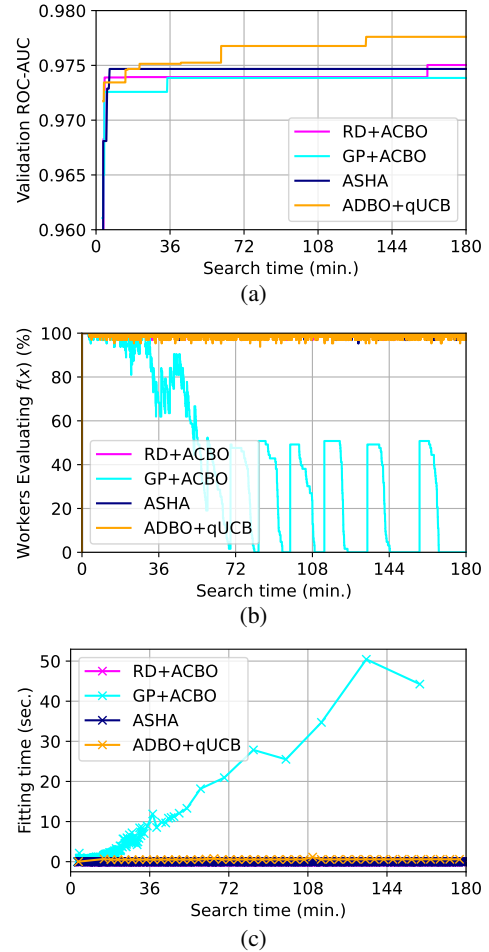


Fig. 8: Comparison of hyperparameter search algorithms on the Attn Benchmark.

is converging faster and to a better solution than RD+ACBO, GP+ACBO, and ASHA. The poor performance of GP+ACBO is attributed to the rapidly decreasing worker utilization shown in Fig. 8b. Fig. 8c shows the time required for refitting the model in different methods. While the refitting time is negligible for ADBO+qUCB, RD+ACBO, ASHA, even at a moderate scale of 64 workers, GP+ACBO suffers from high refit cost. Note that this refit time increases over time because of the number of samples available for refit increase over time. Since ASHA and RD+ACBO are based on random sampling, due the curse of dimensionality, they cannot outperform ADBO+qUCB, which uses more intelligent exploration and exploitation strategies.

2) *Combo benchmark*: The Combo benchmark dataset [45] is composed of 220,890 training data points and 55,222 testing data points respectively. Each data point has 3 class of input features: 942 (RNA-Sequence), 3,839 (drug-1 descriptors) and 3,893 (drug-2 descriptors) respectively. The data set size is about 4.2 GB. It is a regression problem with the goal of predicting the growth percentage of cancer cells given a cell line molecular features and the descriptors of two drugs. The validation data is composed of 20% of the training data. The networks are trained for 10 epochs. The validation R^2 coef-

efficient at the last epoch is used as metric for hyperparameter search. The baseline model is composed of 3 inputs each processed by a sub-network of 3 fully connected layers. Then, the outputs of these sub-models are concatenated and input in an other sub-network of 3 layers before the final output. All the fully connected layers have 1000 neurons and ReLU activation. It reaches a validation R^2 of 0.816. The number of neurons and the activation function of each layer are exposed for the hyperparameter search. The search space is defined as follows: number of neurons, activation function, optimizer, global dropout-rate, batch size, learning rate hyperparameters take the same range as in Attn hyperparameter search. A learning rate warmup strategies is activated based on a boolean variable. Accordingly the base learning rate of this warmup strategy is searched in $[10^{-5}, 10^{-2}]$ with a log-uniform prior. Residual connections are created based on a boolean variable. A learning rate scheduler is activated based on boolean variable. Finally, batch-normalization is activated based on boolean variable. This corresponds to 16 hyperparameters. The results for utilization in Fig. 9b and update duration of the surrogate model in Fig. 9c are similar to Attn in Fig. 8b and 8c respectively. The search trajectory shown in Fig. 9 shows that our proposed ADBO+qUCB outperforms RD+ACBO, GP+ACBO, and ASHA. The GP+ACBO also suffered from poor utilization due to quickly increasing model refitting overheads.

VI. CONCLUSION AND FUTURE WORK

We developed an asynchronous distributed Bayesian optimization (ADBO) method that is capable of leveraging thousands of parallel workers on HPC systems. In ADBO, each worker has its own sequential BO that performs only one black-box evaluation at a time and exchanges the evaluation results among all other workers in an asynchronous way using nonblocking MPI operations `isend` and `irecv`. Each BO worker differ from the others with respect to the exploration and exploitation trade-off and use a random forest surrogate model with improved uncertainty quantification capabilities and two methods that seek to reduce refitting time complexity. The proposed asynchronous communication scheme is generic and can be applied to other distributed BO methods.

Our proposed ADBO method seeks to avoid the congestion issues of centralized BO methods. We showed that our proposed ADBO method outperforms a recently proposed state-of-the-art synchronous distributed BO method and the commonly used centralized BO with single manager and multiple workers. By scaling ADBO from 128 to 4,096 parallel workers we demonstrated an improved effective utilization of about 35%, which translates to 1.68x more evaluated configurations on average compared with its synchronous version. We showed the advantage of scaling to improve the quality of the solution and to reduce the time to solution. To address the problem of increasing the dimensionality and not bounding the size of collected input-output configurations, we proposed a method that combines feature reduction and quantile-based undersampling and demonstrated its benefits.

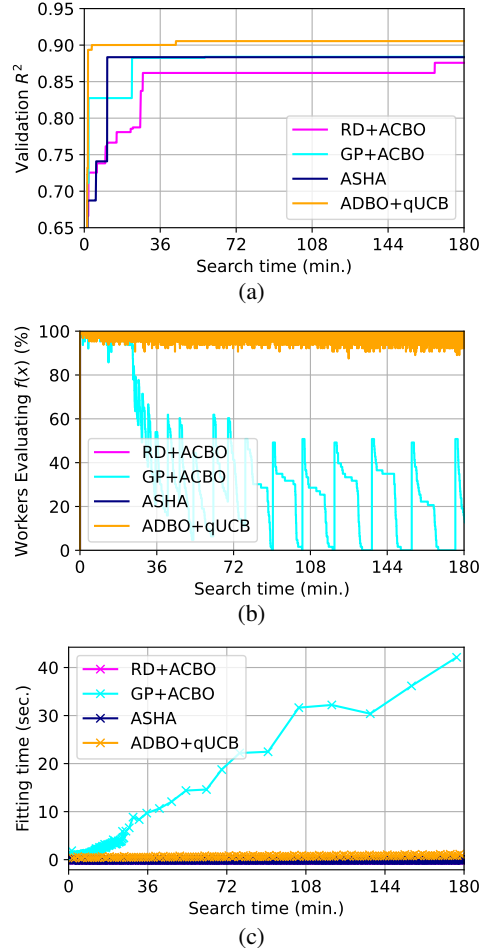


Fig. 9: Comparison of hyperparameter search algorithms for the Combo benchmark.

Finally, we evaluated the efficacy of ADBO for tuning the hyperparameters of a graph neural network and showed that ADBO outperformed a centralized BO method in the state of the art hyperparameter tuning package.

We are making our software open source to benefit the community. We are expanding our study to other relevant areas such as simulation calibration, software tuning, and workflow tuning. Other future work will include 1) the use of accelerators for model refit and related low level system optimization of surrogate model refit, 2) low overhead zeroth-order optimization method to maximize the acquisition function, 3) online dimensional reduction and input domain decomposition, 4) continual/incremental learning surrogate models for ADBO, and 5) multi-objective optimization.

ACKNOWLEDGMENT

This material is based upon work supported by the U.S. Department of Energy (DOE), Office of Science, Office of Advanced Scientific Computing Research, under Contract DE-AC02-06CH11357. This research used resources of the Argonne Leadership Computing Facility, which is a DOE Office of Science User Facility.

REFERENCES

- [1] F. Hutter, H. Hoos, and K. Leyton-Brown, "An efficient approach for assessing hyperparameter importance," in *Proceedings of the 31st International Conference on International Conference on Machine Learning - Volume 32*, ser. ICML'14. JMLR.org, 2014, p. 1–754–1–762.
- [2] S. M. Wild, J. Sarich, and N. Schunck, "Derivative-free optimization for parameter estimation in computational nuclear physics," *Journal of Physics G: Nuclear and Particle Physics*, vol. 42, no. 3, p. 034031, feb 2015. [Online]. Available: <https://doi.org/10.1088%2F0954-3899%2F42%2F3%2F034031>
- [3] F. Hutter, H. H. Hoos, and K. Leyton-Brown, "Sequential model-based optimization for general algorithm configuration," in *International conference on learning and intelligent optimization*. Springer, 2011, pp. 507–523.
- [4] J. S. Bergstra, R. Bardenet, Y. Bengio, and B. Kégl, "Algorithms for Hyper-Parameter Optimization," p. 9.
- [5] M. Hauschild and M. Pelikan, "An introduction and survey of estimation of distribution algorithms," *Swarm and evolutionary computation*, vol. 1, no. 3, pp. 111–128, 2011.
- [6] D. M. Olsson and L. S. Nelson, "The nelder-mead simplex procedure for function minimization," *Technometrics*, vol. 17, no. 1, pp. 45–51, 1975.
- [7] R. Poli, J. Kennedy, and T. Blackwell, "Particle swarm optimization," *Swarm intelligence*, vol. 1, no. 1, pp. 33–57, 2007.
- [8] P.-T. De Boer, D. P. Kroese, S. Mannor, and R. Y. Rubinfeld, "A tutorial on the cross-entropy method," *Annals of operations research*, vol. 134, no. 1, pp. 19–67, 2005.
- [9] T. Bäck and H.-P. Schwefel, "An overview of evolutionary algorithms for parameter optimization," *Evolutionary computation*, vol. 1, no. 1, pp. 1–23, 1993.
- [10] R. A. Rutenbar, "Simulated annealing algorithms: An overview," *IEEE Circuits and Devices magazine*, vol. 5, no. 1, pp. 19–26, 1989.
- [11] B. Shahriari, K. Swersky, Z. Wang, R. P. Adams, and N. de Freitas, "Taking the Human Out of the Loop: A Review of Bayesian Optimization," *Proceedings of the IEEE*, vol. 104, no. 1, pp. 148–175, Jan. 2016. [Online]. Available: <https://ieeexplore.ieee.org/document/7352306/>
- [12] B. Bischl, J. Richter, J. Bossek, D. Horn, J. Thomas, and M. Lang, "ml-rmbo: A modular framework for model-based optimization of expensive black-box functions," *arXiv preprint arXiv:1703.03373*, 2017.
- [13] T. Bartz-Beielstein, "A survey of model-based methods for global optimization," *Bioinspired Optimization Methods and Their Applications*, pp. 1–18, 2016.
- [14] S. Heldens, P. Hijma, B. V. Werkhoven, J. Maassen, A. S. Z. Belloum, and R. V. Van Nieuwpoort, "The landscape of exascale research: A data-driven literature analysis," *ACM Comput. Surv.*, vol. 53, no. 2, mar 2020. [Online]. Available: <https://doi.org/10.1145/3372390>
- [15] J. Bergstra, R. Bardenet, Y. Bengio, and B. Kégl, "Algorithms for hyper-parameter optimization," in *Proceedings of the 24th International Conference on Neural Information Processing Systems*, ser. NIPS'11. Red Hook, NY, USA: Curran Associates Inc., 2011, p. 2546–2554.
- [16] J. Bergstra, D. Yamins, and D. Cox, "Making a science of model search: Hyperparameter optimization in hundreds of dimensions for vision architectures," in *International conference on machine learning*. PMLR, 2013, pp. 115–123.
- [17] A. Klein, S. Falkner, S. Bartels, P. Hennig, and F. Hutter, "Fast Bayesian optimization of machine learning hyperparameters on large datasets," in *Artificial intelligence and statistics*. PMLR, 2017, pp. 528–536.
- [18] P. I. Frazier, "A Tutorial on Bayesian Optimization," *arXiv:1807.02811 [cs, math, stat]*, Jul. 2018, arXiv: 1807.02811. [Online]. Available: <http://arxiv.org/abs/1807.02811>
- [19] J. M. Hernández-Lobato, J. Requeima, E. O. Pyzer-Knapp, and A. Aspuru-Guzik, "Parallel and Distributed Thompson Sampling for Large-scale Accelerated Exploration of Chemical Space," p. 10.
- [20] J. Garcia-Barcos and R. Martinez-Cantin, "Fully Distributed Bayesian Optimization with Stochastic Policies," *arXiv:1902.09992 [cs, stat]*, Jul. 2019, arXiv: 1902.09992. [Online]. Available: <http://arxiv.org/abs/1902.09992>
- [21] P. Balaprakash, M. Salim, T. D. Uram, V. Vishwanath, and S. M. Wild, "DeepHyper: Asynchronous hyperparameter search for deep neural networks," in *2018 IEEE 25th International Conference on High Performance Computing (HiPC)*, 2018, pp. 42–51.
- [22] L. Li, K. Jamieson, G. DeSalvo, A. Rostamizadeh, and A. Talwalkar, "Hyperband: A Novel Bandit-Based Approach to Hyperparameter Optimization," *arXiv:1603.06560 [cs, stat]*, Jun. 2018, arXiv: 1603.06560. [Online]. Available: <http://arxiv.org/abs/1603.06560>
- [23] J. González, Z. Dai, P. Hennig, and N. D. Lawrence, "Batch Bayesian Optimization via Local Penalization," *arXiv:1505.08052 [stat]*, Oct. 2015, arXiv: 1505.08052. [Online]. Available: <http://arxiv.org/abs/1505.08052>
- [24] J. Snoek, H. Larochelle, and R. P. Adams, "Practical Bayesian Optimization of Machine Learning Algorithms," *arXiv:1206.2944 [cs, stat]*, Aug. 2012, arXiv: 1206.2944. [Online]. Available: <http://arxiv.org/abs/1206.2944>
- [25] A. Alvi, B. Ru, J.-P. Calliess, S. Roberts, and M. A. Osborne, "Asynchronous batch Bayesian optimisation with improved local penalisation," in *Proceedings of the 36th International Conference on Machine Learning*, ser. Proceedings of Machine Learning Research, K. Chaudhuri and R. Salakhutdinov, Eds., vol. 97. PMLR, 09–15 Jun 2019, pp. 253–262. [Online]. Available: <https://proceedings.mlr.press/v97/alvi19a.html>
- [26] H. Liu, Y.-S. Ong, X. Shen, and J. Cai, "When Gaussian Process Meets Big Data: A Review of Scalable GPs," *arXiv:1807.01065 [cs, stat]*, Apr. 2019, arXiv: 1807.01065. [Online]. Available: <http://arxiv.org/abs/1807.01065>
- [27] J. Snoek, O. Rippel, K. Swersky, R. Kiros, N. Satish, N. Sundaram, M. M. A. Patwary, Prabhath, and R. P. Adams, "Scalable Bayesian Optimization Using Deep Neural Networks," *arXiv:1502.05700 [stat]*, Jul. 2015, arXiv: 1502.05700. [Online]. Available: <http://arxiv.org/abs/1502.05700>
- [28] F. Hutter, L. Xu, H. H. Hoos, and K. Leyton-Brown, "Algorithm Runtime Prediction: Methods & Evaluation," *arXiv:1211.0906 [cs, stat]*, Oct. 2013, arXiv: 1211.0906. [Online]. Available: <http://arxiv.org/abs/1211.0906>
- [29] J. Mockus, V. Tiesis, and A. Zilinskas, "The application of bayesian methods for seeking the extremum," *Towards global optimization*, vol. 2, no. 117-129, p. 2, 1978.
- [30] J. Larson, M. Menickelly, and S. M. Wild, "Derivative-free optimization methods," *Acta Numerica*, vol. 28, pp. 287–404, 2019.
- [31] L. Breiman, "Random forests," *Machine learning*, vol. 45, no. 1, pp. 5–32, 2001.
- [32] J. T. Wilson, F. Hutter, and M. P. Deisenroth, "Maximizing acquisition functions for Bayesian optimization," *arXiv:1805.10196 [cs, stat]*, Dec. 2018, arXiv: 1805.10196. [Online]. Available: <http://arxiv.org/abs/1805.10196>
- [33] D. Ginsbourger, R. L. Riche, and L. Carraro, "Kriging is well-suited to parallelize optimization," in *Computational intelligence in expensive optimization problems*. Springer, 2010, pp. 131–162.
- [34] F. Pedregosa, G. Varoquaux, A. Gramfort, V. Michel, B. Thirion, O. Grisel, M. Blondel, P. Prettenhofer, R. Weiss, V. Dubourg, J. Vanderplas, A. Passos, D. Cournapeau, M. Brucher, M. Perrot, and E. Duchesnay, "Scikit-learn: Machine learning in Python," *Journal of Machine Learning Research*, vol. 12, pp. 2825–2830, 2011.
- [35] M. P. Forum, "Mpi: A message-passing interface standard," USA, Tech. Rep., 1994.
- [36] P. Balaprakash, R. Egele, M. Salim, V. Vishwanath, and S. M. Wild, "DeepHyper: Scalable Asynchronous Neural Architecture and Hyperparameter Search for Deep Neural Networks," 2018–2022. [Online]. Available: <https://github.com/deephyper/deephyper>
- [37] T. Akiba, S. Sano, T. Yanase, T. Ohta, and M. Koyama, "Optuna: A next-generation hyperparameter optimization framework," 2019. [Online]. Available: <https://arxiv.org/abs/1907.10902>
- [38] Y. Liu, R. Hu, A. Kraus, P. Balaprakash, and A. Obabko, "Data-driven modeling of coarse mesh turbulence for reactor transient analysis using convolutional recurrent neural networks," *Nuclear Engineering and Design*, vol. 390, p. 111716, 2022. [Online]. Available: <https://www.sciencedirect.com/science/article/pii/S002954932200070X>
- [39] R. Égelé, P. Balaprakash, I. Guyon, V. Vishwanath, F. Xia, R. Stevens, and Z. Liu, "AgEBO-Tabular: Joint neural architecture and hyperparameter search with autotuned data-parallel training for tabular data," in *Proceedings of the International Conference for High Performance Computing, Networking, Storage and Analysis*, ser. SC '21. New York, NY, USA: Association for Computing Machinery, 2021. [Online]. Available: <https://doi.org/10.1145/3458817.3476203>
- [40] R. Egele, R. Maulik, K. Raghavan, P. Balaprakash, and B. Lusch, "AutoDEUQ: Automated deep ensemble with uncertainty

- quantification,” *CoRR*, vol. abs/2110.13511, 2021. [Online]. Available: <https://arxiv.org/abs/2110.13511>
- [41] Y. Liu, R. Hu, D. Dai, P. Balaprakash, and A. Obabko, “Machine learning assisted safety modeling and analysis of advanced reactors,” Argonne National Lab.(ANL), Argonne, IL (United States), Tech. Rep., 2021.
- [42] L. Li, K. Jamieson, A. Rostamizadeh, E. Gonina, M. Hardt, B. Recht, and A. Talwalkar, “A System for Massively Parallel Hyperparameter Tuning,” *arXiv:1810.05934 [cs, stat]*, Mar. 2020, arXiv: 1810.05934. [Online]. Available: <http://arxiv.org/abs/1810.05934>
- [43] J. M. Wozniak, R. Jain, P. Balaprakash, J. Ozik, N. T. Collier, J. Bauer, F. Xia, T. Brettin, R. Stevens, J. Mohd-Yusof *et al.*, “Candle/supervisor: A workflow framework for machine learning applied to cancer research,” *BMC bioinformatics*, vol. 19, no. 18, pp. 59–69, 2018.
- [44] A. Clyde, T. Brettin, A. Partin, M. Shaulik, H. Yoo, Y. Evrard, Y. Zhu, F. Xia, and R. Stevens, “A systematic approach to featurization for cancer drug sensitivity predictions with deep learning,” *arXiv preprint arXiv:2005.00095*, 2020.
- [45] F. Xia, M. Shukla, T. Brettin, C. Garcia-Cardona, J. Cohn, J. E. Allen, S. Maslov, S. L. Holbeck, J. H. Doroshov, Y. A. Evrard, E. A. Stahlberg, and R. L. Stevens, “Predicting tumor cell line response to drug pairs with deep learning,” *BMC Bioinformatics*, vol. 19, no. S18, p. 486, Dec. 2018. [Online]. Available: <https://bmcbioinformatics.biomedcentral.com/articles/10.1186/s12859-018-2509-3>